CHEMISTRY OF MATERIALS

COMMUNICATION

pubs.acs.org/cm

Efficient Deep-Blue Electroluminescence from an Ambipolar Fluorescent Emitter in a Single-Active-Layer Device

Alison L. Fisher,[†] Katharine E. Linton,[‡] Kiran T. Kamtekar,[‡] Christopher Pearson,[†] Martin R. Bryce,*[,‡] and Michael C. Petty*[,†]

[†]School of Engineering and [‡]Department of Chemistry, Durham University, Durham, DH1 3LE, United Kingdom

Supporting Information

KEYWORDS: optical materials

Organic light-emitting devices (OLEDs) offer great potential for applications in flat panel displays[1] and solid-state lighting.[2] A wide variety of efficient red- and green-emitting organic materials have been developed. However, there are far fewer stable blue-emitting materials which are required for full-color displays and as components for generating white light. Due to their intrinsically larger HOMO−LUMO gap, blue emitters can also be utilized to generate emission of other colors by energy transfer, serving as hosts for lower energy dopant emitters. As noted recently by Reynolds et al.[3] and Wong et al.,[4] only a handful of deep-blue OLEDs based on organic fluorescent emitters achieve external quantum efficiences (EQEs) greater than 1%. Examples of molecules for blue-emitting OLEDs are derivatives of anthracene,[5] carbazole,[6] and fluorene.[7] However, these units are predominantly hole transporters, and a key requirement for an efficient electroluminescent device is balanced hole and electron transport.[8] Therefore, ambipolar molecules with the propensity to stabilize both positive and negative charges are attractive candidates. A range of donor−acceptor (D−A) systems have been explored to manipulate the HOMO−LUMO levels and the emission color. D−A combinations include triarylamine−quinoline,[9] phenoxazine−quinoline,[10] diphenylamine−diazaspirobifluorene,[11] triarylamine−1,3,4-diaryloxadiazole,[12] and carbazole−1,3,4-diaryloxadiazole.[13] Alternative acceptor units in D−A systems include diarylboron,[14] benzothiadiazole,[15] dibenzothiophene-*S*,*S*-dioxide,[16] and benzimidazole.[17]

In this context, we previously reported the ambipolar molecule **1**, Figure 1, and its use, in the form of a spin-coated film, as an emitter in the OLED architecture indium−tin oxide (ITO)/poly(3,4-ethylenedioxythiophene):poly(styrenesulfonate) (PEDOT:PSS)/**1**/Ca/Al.[12b] We now report that the new carbazole analogue **2** exhibits significantly improved device performance, notably highly saturated deep-blue emission (CIEy < 0.10) with a maximum EQE of 4.7% in a single-active-layer device architecture.

The synthesis of **2** is reported in the Supporting Information.

The OLED architecture was similar to that used in our previous work,[12b] that is, ITO/PEDOT-PSS/**2**/Ca/Al The device fabrication and measurement procedures are provided in the Supporting Information. To allow comparison of devices of differing size, the current and photocurrent data have been converted to current density and photocurrent density. The current density versus electric field (J−E), photocurrent density versus electric field (J_{ph}−E), and EQE characteristics for **1** and **2** are given in Figures 2 and 3.

From Figure 2a, it is evident that the conductivity of **1** is greater than that of **2**. It is expected that the HOMO level will be lowered when the diphenylamino group of **1** is replaced by a carbazole group. This is confirmed by the DFT calculations in the Supporting Information. An increase of around 0.4 eV is predicted for the energy barrier for holes from the ITO/PEDOT anode into the emitter layer. Although we do not have independent values for the carrier concentrations or mobilities of our compounds, the conductivity data are consistent with holes being the majority carriers in both compounds. Figure 2b reveals a smaller photocurrent per unit electric field for **2**. However, J_{ph} is not reduced as much as J. We suggest that the improved balance between the electron and hole current for **2** leads to the significant increase in the EQE, as shown in Figure 3. A fivefold enhancement in EQE is achieved, from 0.26% for **1** to 1.25% in the case of analogue **2**.

Figure 4a compares the electroluminescence (EL) spectra for **1** and **2**, revealing a blue shift of around 56 nm in the emission of **2** relative to **1**. For **1**, the peak emission is 487 nm while for **2** peak emission occurs at a lower wavelength of 431 nm. This shift suggests an increased HOMO−LUMO separation for compound **2**. Again, this is confirmed by the DFT calculations which show a HOMO−LUMO separation of 3.48 eV for **2** in comparison with 3.22 eV for **1**.

The shape of the emission spectra also varies slighly between the two analogues, with **1** exhibiting three main peaks at 458 nm, 487 nm, and 517 nm together with a shoulder at around 555 nm. In contrast, compound **2** shows four peaks at 413 nm, 431 nm, 452 nm, and 480 nm and a shoulder at approximately 520 nm.

The blue shift for **2** becomes further apparent on inspection of the Commission Internationale de L'Eclairage (CIE) diagram, Figure 4b. Compound **2** shows a particularly saturated deep blue emission (0.156, 0.069) compared to **1** (0.191, 0.352). This is very close to the National Television System Committee (NTSC) standard blue CIE coordinates of (0.14, 0.08).[4] A photograph of the light output from an OLED of **2** is given as an inset in the CIE diagram. Some preliminary data indicating an improved stability for unencapsulated OLEDs based on **2** are provided in the Supporting Information.

Received: November 18, 2010
Revised: March 1, 2011
Published: March 14, 2011

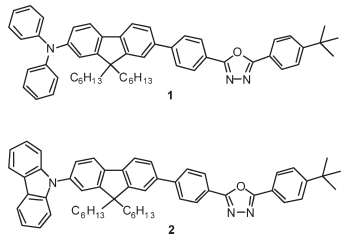

Figure 1. Structures of compounds **1** and **2**.

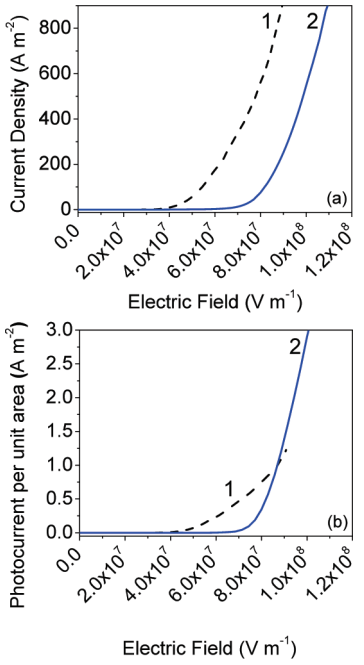

Figure 2. (a) Current density as a function of electric field; (b) photocurrent per unit area as a function of electric field. Active layers in OLEDs produced by spin-coating.

The effects on the behavior of the OLEDs of using spin-coating and thermal evaporation to deposit the emissive layer are contrasted in Table 1 (data for the spin-coated device incorporating **1** have been taken from measurements of a device from a previous study[12b]). We do not believe that the small variations in thickness explain the differences in EQE. For both **1** and **2** the use of evaporated layers enhances the device EQE. Furthermore, the current and power efficiencies are both improved for **2** in the form of an evaporated layer. The efficiencies of our single-active-layer devices compare very favorably with those reported for multilayer blue emitting devices based on ambipolar compounds.[14b]

The surface morphologies of the different layers used in this study are shown by the atomic force microscopy (AFM) images in Figure 5. Relatively smooth, apparently amorphous surfaces are evident for the spin-coated layers of both compounds, Figure 5a,c. However, distinct grains are apparent in the AFM images of the evaporated materials, Figure 5b,d.

Photoluminescene measurements (provided in the Supporting Information) reveal no major differences in the fluorescence quantum efficiencies for the films in their different morphological forms. The polycrystalline structure of the thermally evaporated organic layers should lead to improved carrier mobilities for both holes and electrons. Devices based on the evaporated emitters were

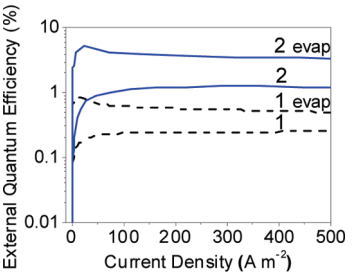

Figure 3. External quantum efficiencies of **1** and **2**. Data are shown for OLEDs in which the active layer has been deposited by both spin-coating and thermal evaporation (data denoted as **1** evap and **2** evap).

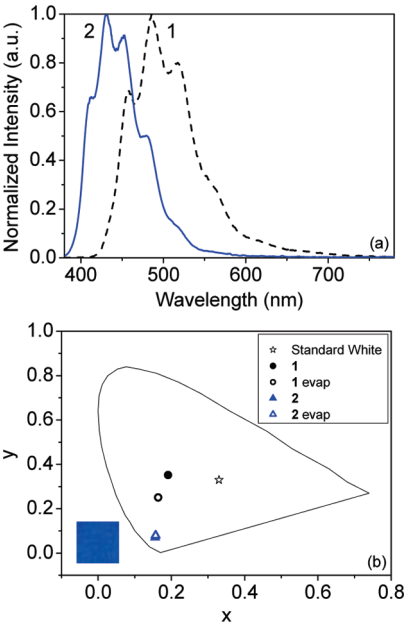

Figure 4. (a) EL spectra of devices based on spin-coated layers of **1** and on **2**; (b) comparison of CIE coordinates of devices comprising **1** and **2**, measured at $J \sim 150$ A m^{-2} for **1** and $J \sim 50$ A m^{-2} for **2**. Active layers in OLEDs produced by spin-coating and thermal evaporation. Inset is a photograph of the deep-blue OLED of **2**.

found to possess a significantly higher conductivity than those fabricated by spin-coating (data provided in the Supporting Information). We suggest that the electron mobility is enhanced more than the hole mobility, leading to a better balance between the electron and hole currents and, consequently, to the increase in the efficiency. Additionally, the emission zone may be moved further away from the Ca/Al cathode, reducing EL quenching effects.

Table 1 also indicates that the efficiencies of **2** are improved more (ca. 4 times in the case of the EQE) than those of **1** (ca. 2.5 times for the EQE) by using thermal evaporation. While the different processing methods have little influence on the color of the OLEDs incorporating **2**, the evaporated OLEDs containing **1** reveal a blue shift in the CIE coordinates when compared to devices fabricated using spin-coating (Figure 4b). This is possibly related to microcavity effects resulting from the different film thicknesses.

In summary, the new ambipolar molecule **2** has been successfully integrated into a simple, single-active-layer OLED to produce devices which are among the highest performing deep-blue OLEDs. Using thermal evaporation to produce layers of **2** an EQE of over 4% with

dx.doi.org/10.1021/cm103314t |*Chem. Mater.* 2011, 23, 1640–1642

Table 1. Comparison of Characteristics of the Spin-Coated and Evaporated Devices

compound	deposition method	emissive layer thickness (nm)	peak emission (nm)	fwhm (nm)	CIE[a] x	CIE[a] y	turn-on electric field (V m^{-1}) (turn-on voltage, V)	EQE[b] (%)	current efficiency[c] (cd A^{-1})	power efficiency[c] (lm W^{-1})	brightness[c] (cd m^{-2})
1	spin-coated	110	487	87	0.191	0.352	2.96×10^7 (3.53)	0.26			
1	evaporated	70	484	105	0.164	0.251	6.24×10^7 (4.30)	0.63	0.93	0.30	943.2
2	spin-coated	70	431	67	0.156	0.069	4.50×10^7 (3.15)	1.25	0.47	0.18	483.1
2	evaporated	105	431	81	0.157	0.079	3.99×10^7 (4.18)	4.71	1.49	0.53	1520.0

[a] CIE coordinates of spin-coated **1** measured at an applied current of 0.5 mA ($J \sim 150$ A m^{-2}). All other OLEDs measured at an applied current of 1 mA ($J \sim 50$ A m^{-2}). [b] EQE measured at 100 ± 30 cd m^{-2}. [c] Measured under an applied current of 20 mA ($J \sim 10^3$ A m^{-2}).

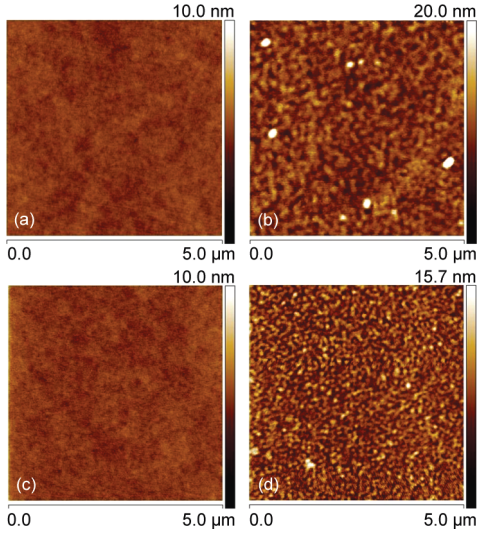

Figure 5. AFM images of films of (a) spin-coated **1** (film thickness = 53 nm); (b) evaporated **1** (64 nm); (c) spin-coated **2** (61 nm); and (d) evaporated **2** (59 nm).

CIE coordinates of (0.157, 0.079) has been achieved. This combination of highly efficient deep-blue emission and a simple device architecture is very attractive for further development.

■ ASSOCIATED CONTENT

Supporting Information. Experimental procedures and characterization data; device configuration; OLED stability data; solution photophysical and electrochemical data; photoluminescence data; DFT calculations (PDF).This material is available free of charge via the Internet at http://pubs.acs.org.

■ AUTHOR INFORMATION

Corresponding Author

*E-mail: m.r.bryce@durham.ac.uk (M.R.B.); m.c.petty@durham.ac.uk (M.C.P.).

■ ACKNOWLEDGMENT

We thank EPSRC for funding, Dr. M.A. Fox for the DFT calculations, and Dr L.-O. Pålsson for photoluminescence data of thin films.

■ REFERENCES

(1) (a) Grimsdale, A. C.; Chan, K. L.; Martin, R. E.; Jokisz, P. G.; Holmes, A. B. *Chem. Rev.* **2009**, *109*, 897–1091.(b) Kakafi, Z. H. *Organic Electroluminescence*; CRC Press: New York, NY, 2005. (c) Müllen, K.; Scherf, U. *Organic Light-Emitting Devices*; Wiley-VCH: Weinheim, Germany, 2006. (d) Li, Z.; Meng, H. *Organic Light-Emitting Materials and Devices*; CRC Press: Boca Raton, FL, 2006.

(2) (a) Kamtekar, K. T.; Monkman, A. P.; Bryce, M. R. *Adv. Mater.* **2010**, *22*, 572–582. (b) Beaupré, S.; Boudrealt, P.-L. T.; Leclerc, M. *Adv. Mater.* **2010**, *22*, E6–E27.

(3) Yang, Y.; Cohn, P.; Dyer, A. L.; Eom, S.-H.; Reynolds, J. R.; Castellano, R. K.; Xue, J. *Chem. Mater.* **2010**, *22*, 3580–3582.

(4) Tsai, T.-C.; Hung, W.-Y.; Chi, L.-C.; Wong, K.-T.; Hseih, C.-C.; Chou, P.-T. *Org. Electron.* **2009**, *10*, 158–162.

(5) Lee, M. T.; Chen, H. H.; Liao, C. H.; Tsai, C. H.; Chen, C. H. *Appl. Phys. Lett.* **2004**, *85*, 3301–3303.

(6) Tong, Q.-X.; Lai, S.-L.; Chan, M.-Y.; Zhou, Y.-C.; Kwong, H.-L.; Lee, C.-S.; Lee, S.-T. *Chem. Mater.* **2008**, *20*, 6310–6312.

(7) Zhen, C.-G.; Chen, Z.-K.; Liu, Q.-D.; Dai, Y.-F.; Shin, R. Y. C.; Chang, S.-Y.; Kieffer, J. J. *Adv. Mater.* **2009**, *21*, 2415–2429.

(8) (a) Kulkarni, A. P.; Tonzola, C. J.; Babel, A.; Jenekhe, S. A. *Chem. Mater.* **2004**, *16*, 4556–4573. (b) Hughes, G.; Bryce, M. R. *J. Mater. Chem.* **2005**, *15*, 94–107. (c) Shirota, Y.; Kageyama, H. *Chem. Rev.* **2007**, *107*, 953–1010. (d) Tamoto, N.; Adachi, C.; Nagai, K. *Chem. Mater.* **1997**, *9*, 1077–1085.

(9) Hancock, J. M.; Gifford, A. P.; Zhu, Y.; Lou, Y.; Jenekhe, S. A. *Chem. Mater.* **2006**, *18*, 4924–4932.

(10) (a) Zhu, Y.; Kulkarni, A. P.; Wu, P.-T.; Jenekhe, S. A. *Chem. Mater.* **2008**, *20*, 4200–4211. (b) Kulkarni, A. P.; Zhu, Y.; Babel, A.; Wu, P. T.; Jenekhe, S. A. *Chem. Mater.* **2008**, *20*, 4212–4223.

(11) Chi, C.-C.; Chiang, C.-L.; Liu, S.-W.; Yueh, H.; Chen, C.-T.; Chen, C.-T. *J. Mater. Chem.* **2009**, *19*, 5561–5571.

(12) (a) Patra, A.; Pan, M.; Friend, C. S.; Lin, T.-C.; Cartwright, A. N.; Prasad, P. N. *Chem. Mater.* **2002**, *14*, 4044–4048. (b) Kamtekar, K. T.; Wang, C.; Bettington, S.; Batsanov, A. S.; Perepichka, I. F.; Bryce, M. R.; Ahn, J. H.; Rabinal, M.; Petty, M. C. *J. Mater. Chem.* **2006**, *16*, 3823–3835.

(13) Thomas, K. R. J.; Linn, J. T.; Tao, Y.-T.; Chuen, C.-H. *Chem. Mater.* **2004**, *16*, 5437–5444.

(14) (a) Doi, H.; Kinoshita, M.; Okumoto, K.; Shirota, Y. *Chem. Mater.* **2003**, *15*, 1080–1089. (b) Zhang, H.; Huo, C.; Zhang, J.; Zhang, P.; Tian, W.; Wang, Y. *Chem. Commun.* **2006**, 281–283. (c) Lin, S.-L.; Chan, L.-H.; Lee, R.-H.; Yen, M.-Y.; Kuo, W.-J.; Chen, C.-T.; Jeng, R.-J. *Adv. Mater.* **2008**, *20*, 3947–3952.

(15) Thomas, K. R. J.; Lin, J. T.; Velusamy, M.; Tao, Y.-T.; Chuen, C.-H. *Adv. Funct. Mater.* **2004**, *14*, 83–90.

(16) Huang, T.-H.; Lin, J. T.; Chen, L.-Y.; Lin, Y.-T.; Wu, C.-C. *Adv. Mater.* **2006**, *18*, 602–606.

(17) Lai, M.-Y.; Chen, C.-H.; Huang, W.-S.; Lin, J. T.; Ke, T.-H.; Chen, L.-Y.; Tsai, M.-H.; Wu, C.-C. *Angew. Chem., Int. Ed.* **2008**, *47*, 581–585.